Available online at www.sciencedirect.com
SCIENCE DIRECT®
International Journal of Heat and Mass Transfer 47 (2004) 5439–5450
International Journal of HEAT and MASS TRANSFER
www.elsevier.com/locate/ijhmt

Forced convection and flow friction characteristics of air-cooled horizontal equilateral triangular ducts with ribbed internal surfaces

D.D. Luo, C.W. Leung *, T.L. Chan

Department of Mechanical Engineering, The Hong Kong Polytechnic University, Hung Hom, Kowloon, Hong Kong, PR China

Received 19 September 2003; received in revised form 2 July 2004
Available online 16 September 2004

Abstract

Experimental studies have been conducted to examine the forced convection and flow friction characteristics of air-cooled horizontal equilateral triangular ducts whose internal surfaces have been fabricated with uniformly spaced square ribs. Effects of duct geometry (i.e. relative rib height (H/D) and relative rib-to-rib spacing (S/W)) as well as the hydraulic-diameter based Reynolds number (Re_D) on heat transfer coefficient and friction factor of a fully developed turbulent air flow in a horizontal triangular duct with ribbed internal surfaces have been fully investigated. The ranges of experimental parameters under consideration are: H/D from 0.11 to 0.21, S/W from 3.41 to 13.93, and Re_D from 4000 to 23,000. Optimum relative rib height and relative rib-to-rib spacing corresponding to maximum thermal performance of this system have been determined, which are equal to 0.18 and 7.22, respectively. Flow friction in the triangular duct increases rather linearly with the relative rib height, but a maximum flow friction factor is obtained at the relative rib-to-rib spacing of 7.22. Non-dimensional expressions for prediction of average Nusselt number and friction factor in terms of Re_D, H/D and S/W have been developed correspondingly, which correlate well with the experimental data with maximum deviations of ±3.5% and ±8.7%, respectively.

1. Introduction

Ducts with non-circular cross-section are widely used in many industrial applications such as compact heat exchangers, air conditioners, heat pumps, refrigeration systems, nuclear reactors, etc, which need to be very compact on the one hand, and to transfer heat rapidly to the environment to ensure their proper functioning on the other hand. In fact, thermal performance of a duct will be reduced when the circular cross-sectional shape is not used. However, it is able to enhance the forced convection, which is the major heat transfer mechanism, in a non-circular duct by applying artificially roughened internal surfaces to promote local turbulence. Such effective artificial roughness can be produced by machining processes such as milling, shaping, casting and sand blasting, or fixing ribs or cutting grooves uniformly along the axial length of the duct. Kang et al. [1] had compared the thermal performance of several kinds of artificial roughness elements, which were processed on the internal surfaces of a triangular duct, and suggested that the ribbed surface was able to

* Corresponding author. Tel.: +852 2766 6651; fax: +852 2365 4703.
E-mail address: mmcwl@polyu.edu.hk (C.W. Leung).

0017-9310/$ - see front matter © 2004 Elsevier Ltd. All rights reserved.
doi:10.1016/j.ijheatmasstransfer.2004.07.003

Nomenclature

A	internal surface area of the triangular duct (m^2)
A_c	cross-sectional area of the triangular duct (m^2)
A_0, A_1	coefficients in Eq. (13)
B_0, B_1, B_2	coefficients in Eq. (14)
C_0, C_1, C_2	coefficients in Eq. (15)
D	hydraulic diameter of the triangular duct (mm)
$\dot{E}$	electric power supplied to heat the triangular duct (W)
E_s	standard pumping power per unit heat transfer area ($W m^{-2}$)
f	average friction factor
F	view factor for thermal radiation from the duct ends to its surroundings
h	average convective heat transfer coefficient at the air/duct interface ($W m^{-2} K^{-1}$)
H	rib height (mm)
k	thermal conductivity of the air ($W m^{-1} K^{-1}$)
L	axial length of the triangular duct (mm)
$\dot{m}$	mass flow rate ($kg s^{-1}$)
Nu_D	hydraulic diameter based average Nusselt number of the airflow
P	fluid pressure (Pa)
Pr	Prandtl number of the air
$\dot{Q}_c$	steady-state forced convection from the triangular duct to the airflow (W)
$\dot{Q}_l$	conduction heat loss from the external surfaces of the triangular duct to the surroundings (W)
$\dot{Q}_r$	radiation heat loss from both ends of the triangular duct to the surroundings (W)
Re_D	hydraulic diameter based Reynolds number of the airflow
S	rib-to-rib spacing (mm)
T	temperature (K)
T_a	mean temperature of the airflow (K)
T_s	mean surface temperature of the triangular duct (K)
T_∞	ambient temperature (K)
U	mean velocity of the airflow in the triangular duct ($m s^{-1}$)
W	rib width (mm)

Greek symbols

ε_r	mean surface-emissivity with respect to thermal radiation
μ	dynamic viscosity of the air ($kg m^{-1} s^{-1}$)
ν	kinematic viscosity of the air ($m^2 s^{-1}$)
ρ	density of the air ($kg m^{-3}$)
σ	Stefan–Boltzmann constant ($W m^{-2} K^{-4}$)

Subscripts

a	air
i	inlet plane of the triangular duct
o	outlet plane of the triangular duct
s	triangular duct internal surface
w	wall

produce a significant enhancement in heat transfer. However, use of roughened internal surfaces normally leads to a higher flow friction and hence a higher axial pressure drop along the duct, therefore heat transfer and flow friction characteristics are highly related and should be usually studied simultaneously.

Many investigations have been carried out to study the heat transfer augmentation by using ribbed surfaces under laminar or turbulent flow condition. Ohara et al. [2] conducted an experimental investigation on a narrow vertical channel with ribbed internal surfaces and studied the effect of incorporating repeated transverse rectangular ribs on forced convection heat transfer. Zhang et al. [3] performed a similar test and measured the steady-state heat transfer from rectangular channels with ribbed or grooved internal surfaces. Hong and Hsieh [4] applied different rib alignments, either staggered or in-line, on the internal surfaces of rectangular or square channels, and effect of the rib alignment on forced convection in these channels had been reported. Saini and Saini [5] increased the roughness of the internal surfaces of a rectangular duct by fixing transverse thin circular-sectioned wires in a regular pattern, and conducted an experimental study on the local heat transfer coefficient of the system. Lorenz et al. [6] studied the asymmetrically ribbed channel and investigated the heat transfer coefficient distribution and the pressure drop along the internal wall. Above investigations [2–6] were carried out with square or rectangular cross-sectional ducts under fully developed turbulent condition and constant heat-flux being applied to the channel wall. They came to the same conclusion that forced convection in a rectangular or square duct could be greatly enhanced by fixing ribs uniformly on its internal surfaces.

Considering the limited space in many applications, ducts with triangular cross-sections attract more attention of engineers because of their excellent compactness and very low fabrication cost. Sparrow and Haji-Sheihk

[7] studied the heat transfer and pressure drop characteristics of laminar flows in isosceles-triangular, right-triangular and circular-section ducts. Nakamura et al. [8] investigated forced convection of laminar flow in arbitrary triangular ducts. Hurst and Rapley [9] studied the fully developed turbulent flow in a right-triangular duct with internal angles of 60° and 30°. Hwang and Cheng [10] carried out an experimental study to measure the local heat transfer coefficients and static pressure drops in a leading-edge triangular duct cooled by impinging jets. Schmidt and Newell [11] and Schneider and LeDain [12] studied the forced convection in equilateral triangular cross-sectional smooth ducts under fully developed laminar flow condition. Altemani and Sparrow [13] developed a relationship between fluid friction and forced convection for the same system under turbulent flow condition: two walls were provided with uniform heat flux along their axial length whereas the third wall was thermally insulated. Braga and Saboya [14] used a similar heating arrangement to [13] and studied the heat transfer and fluid friction characteristics of equilateral triangular ducts. Leung and Probert [15] investigated the effect of apex angle of isosceles triangular duct on forced convection of a turbulent flow through the duct, and recommended that 60° was the optimum apex angle corresponding to a maximum forced convection. In addition, an experimental study on the effect of roughened internal surfaces on forced convection and flow friction in horizontal triangular ducts [16] verified that a higher forced convection could be achieved by applying artificially roughened internal surfaces, especially the ribbed surfaces.

Very few investigations have been conducted to study turbulent heat transfer and flow friction characteristics of the triangular duct fabricated uniformly with ribs on its internal surfaces. Integration of a triangular duct with ribbed surfaces leads to a very complicated system configuration and hence flow regime. Its application is becoming popular, however, information is not yet sufficient to better utilize it to thermal systems. In the present investigation, experimental studies are conducted to fill up this gap. Square ribs are attached on the internal surfaces of a horizontal equilateral triangular duct with a uniform rib-to-rib spacing. Effects of rib size and rib-to-rib spacing, the two most important geometric parameters, on the turbulent forced convection and flow friction characteristics of the triangular duct are fully investigated.

2. Experimental rig

A typical experimental rig of the present investigation is shown schematically in Fig. 1(a). In order to investigate the effects of rib size and rib-to-rib spacing on forced convection and flow friction in a horizontal equilateral triangular duct with uniformly ribbed internal surfaces, several geometrically identical equilateral triangular duct assemblies are fabricated from a 1 mm thick duralumin plate (i.e. thermal conductivity = 180 W/(m K)). Each of these duct assemblies consists of three consecutive triangular sections: a 700 mm long entrance duct, a 1050 mm long test duct and a 700 mm long exit duct. Total length of the entrance duct and the test duct is over 40 times of the hydraulic diameter (i.e. $D = 44$ mm) to ensure a fully developed turbulent airflow in a significant portion of the test section [17]. In addition, the exit duct is used together with the entrance duct to minimize the end effect on the airflow through the test duct. These three sections are all fabricated with sharp corners, and of identical cross-sectional shapes and dimensions, namely, each edge is 76 mm long (as shown in Fig. 1(b)), but they are thermally insulated from each other by the installation of formica sheets, gaskets and seals.

Uniform heating is provided from the electrically heated nichrome wire, which wounds uniformly around the external surfaces of the triangular duct. The electric power ($\dot{E}$) supplied to heat the nichrome wire is monitored by a multi-meter and maintained at 200 W via a variable-voltage transformer throughout every experiment. Since the nichrome wire achieves an excellent efficiency of 99%, nearly all the supplied electric power is therefore converted to heating power. A very thin wall thickness (i.e. 1 mm) is used to achieve an efficient heat transfer from the nichrome wire, which is attached on the outer surfaces, to the inner surfaces of the triangular duct by minimizing the thermal resistance through the duct wall due to conduction. To provide a uniform heat flux through the duct wall and to ensure the same heating power is supplied to each of these triangular ducts under investigation, the separation between two adjacent nichrome wires is maintained at 10 mm throughout the entire axial length of the triangular duct.

The whole triangular duct assembly is thermally insulated from its ambient environment by the sandwich of a 1 mm thick formica sheet, a 8.5 mm thick plywood sheet and a 35 mm thick fiberglass blanket (as shown in Fig. 2). The assembly is supported at two points only so that the entire external surfaces are exposed to the same ambient condition. A level gauge is used to ensure that the assembly has been placed horizontally.

In order to drive the ambient air around 16 °C through the triangular duct, a 550 W centrifugal blower is installed at the exit of the exit duct. The blower exit is connected to a circular pipe by a flexible connecting pipe to facilitate more stable flow rate measurement. The blower is physically isolated from the triangular duct assembly to avoid transmission of its vibration to the assembly. Since the experiments are performed at different flow conditions, electric power supplied to drive the blower is adjusted through a variable-voltage

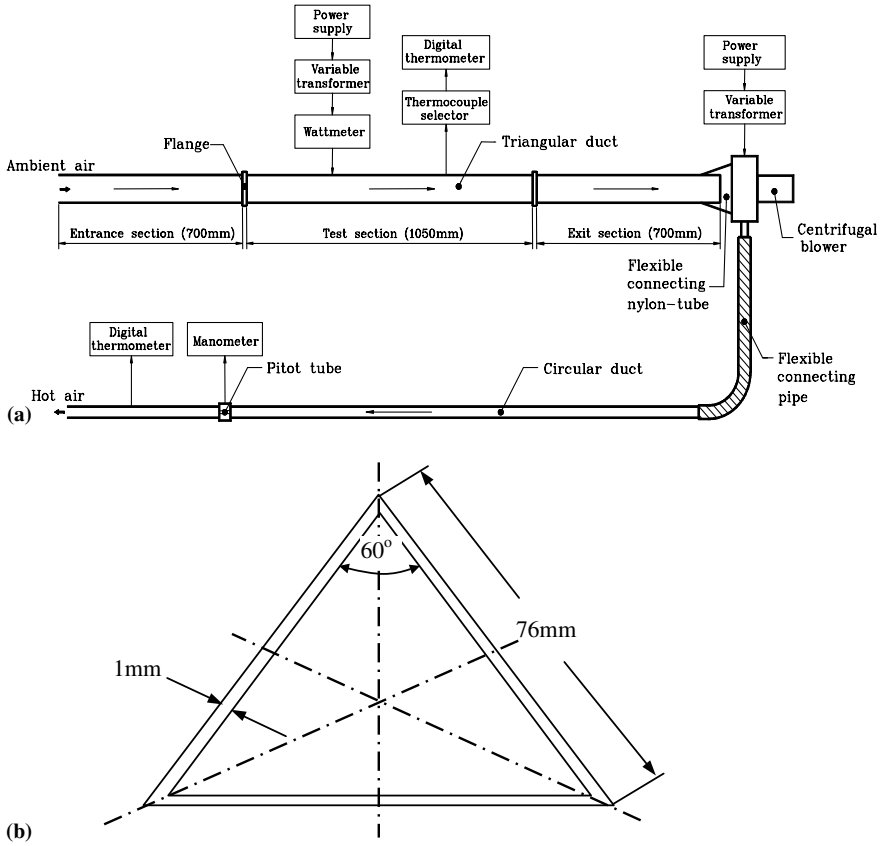

Fig. 1. (a) Experimental set-up of the duct assembly. (b) Dimension of the triangular duct, $D = 44$ mm.

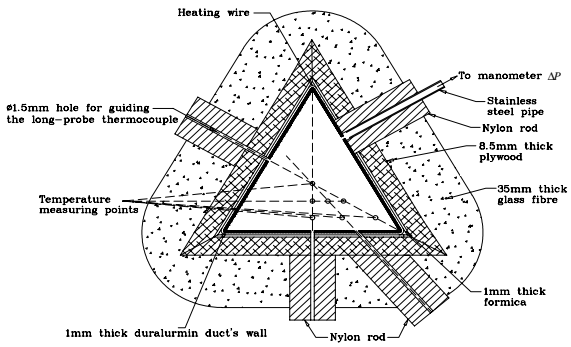

Fig. 2. Locations of temperature measurement in a cross-sectional plane of the triangular duct.

transformer. In order to reduce the extraneous heat loss from the end of the triangular duct assembly to the blower, a thin nylon tube of very low thermal conductivity is employed as their connection. In addition, all connecting parts are joined with gaskets and seals to prevent air leakage and soap bubble is used to test any air leakage at each joint.

Length of the circular pipe is 2230 mm and its diameter is 54 mm. As the ratio of its length and diameter exceeds 40, velocity profile can be determined at a cross-sectional plane around its exit where the flow is already fully developed [1].

3. Experimental measurements and procedure

Uniformly spaced square ribs are fixed on all three internal surfaces of the triangular duct under consideration, as shown in Fig. 3(a). As observed in the previous studies [1,16], the best thermal performance of a ribbed-triangular duct would likely be obtained at a height-to-hydraulic-diameter ratio of the rib (H/D) between 0.10 and 0.22, the rib sizes used in present study are therefore within the range of $H/D = 0.11$ to 0.21, as shown in Table 1. The rib-to-rib-spacing adopted are also provided, which lead to the use of a spacing-to-width ratio of the rib (S/W) between 3.41 and 13.93. The experimental studies are conducted under turbulent flow condition with a wide range of Reynolds numbers from 4000 to 23,000.

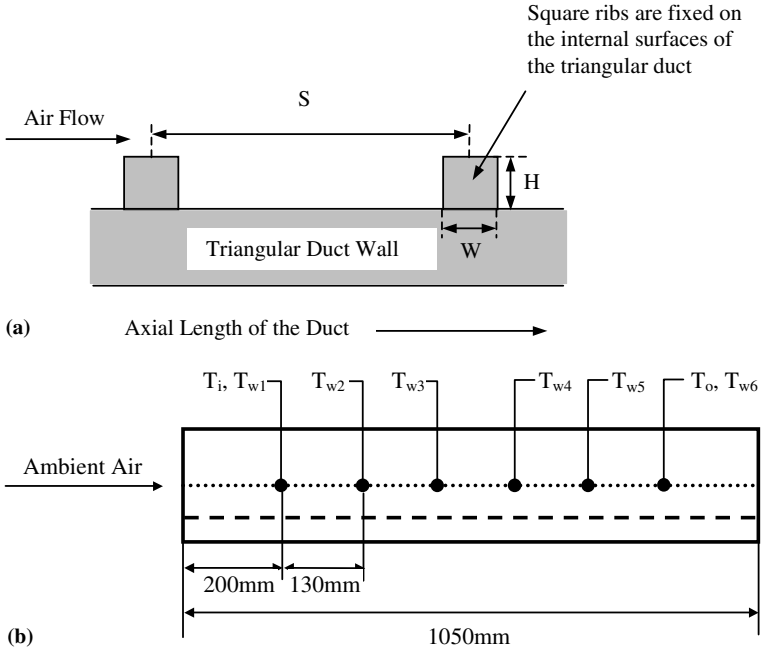

Fig. 3. (a) Schematic representation of the ribbed surface. (b) Locations of temperature measurement along axial length of the triangular duct.

Table 1
Ranges of experimental parameters ($D = 44$ mm)

Configuration	Rib sizes ($H \times W$) (mm) × (mm)	Rib-to-rib spacing (S) (mm)
(**1**)	5 × 5	57
(**2**)	6 × 6	57
(**3**)	7 × 7	57
(**4**)	7.9 × 7.9	27
(**5**)	7.9 × 7.9	47
(**6**)	7.9 × 7.9	57
(**7**)	7.9 × 7.9	67
(**8**)	7.9 × 7.9	75
(**9**)	7.9 × 7.9	110
(**10**)	9 × 9	57

To record the duct's surface temperatures, a digital thermometer is connected with K-type thermocouples, which are installed at six junctions along the axial length of the test duct, as shown in Fig. 3(b). These data are then averaged to give the average internal wall temperature of the test duct (T_s), which is ranging from 345 to 380 K. Because of the excellent thermal conductivity of duralumin, variation in surface temperatures of the entire test duct is less than 10 °C in every test. Each junction consists of three K-type thermocouples installed on the three internal surfaces of the triangular duct at the same cross-sectional plane. Every thermocouple is spot welded and embedded inside a narrow hole of the duct wall, which is perpendicular to the mean airflow direction. Heat transfer compound is applied to fill the residual cavity between the junction and the wall to ensure a good thermal contact. This method enables the point of measurement to be placed closer to the internal surface of the wall, where the temperature readings are more desirable, and more accurate temperature measurement can thus result [13].

Steady-state temperatures of the airflow at entrance and exit of the test duct are measured by a K-type long-probe thermocouple connected to the digital thermometer. Diameter of this long probe thermocouple is only 1.5 mm, so that it will not affect the flow pattern significantly during each measurement. Air temperatures are taken at seven different locations on the same cross-sectional plane (see Fig. 2), which is normal to the airflow direction. Two planes for the measurement are chosen, each of them is 200 mm from entrance and exit of the test duct, respectively. Together with the use of the entrance and exit ducts, such arrangement is able to produce negligible end effect [18]. All K-type thermocouples used in the present investigation have been well pre-calibrated.

For determination of the axial pressure drop (ΔP) along the test duct, two ports fabricated from nylon rods and stainless steel tubes are installed at the same cross-sectional positions where the long-probe thermocouple is applied. The non-leaking pressure taps are connected to a manometer during each measurement, but blocked

off by plugs at all other times in order to prevent air leakage. Each pressure tap has a diameter of 1.5 mm. A cross-sectional view of the triangular test duct showing positions for the temperature and pressure measurements is presented in Fig. 2. In present study, it is assumed that the axial pressure drop along the triangular test duct is entirely due to the flow friction.

Air velocity in the circular pipe is determined using a pitot tube, which is equipped with a manometer, at a location near to the exit of the circular pipe. Velocity measurement is taken at 12 different locations on the same cross-sectional plane, at 2 mm intervals along the pipe radius from its centerline. Accurate positioning of the pitot tube is achieved by using a vertical traversing mechanism mounted on a vernier caliper. A K-type thermocouple, at the exit of the circular pipe, is used to measure the mean air stream temperature, and the atmospheric pressure is obtained from a barometer. By the principle of mass conservation, mass flow rate of air ($\dot{m}$) through the circular pipe is equal to that passing through the triangular duct. Therefore, mass flow rate of air through the triangular duct could be obtained under a less fluctuating condition. The mean air velocity (U) through the triangular duct is then determined by applying the Continuity equation with the aid of the mass flow rate. Overall set-up of the instrumentation is shown in Fig. 1.

4. Deduction of experimental data

Convection heat transfer coefficient from the heated triangular duct to the airflow is obtained from the following relationship:

$$h = \frac{\dot{Q}_c}{A(T_s - T_a)} \tag{1}$$

where the steady-state temperature of the airflow (T_a) is assumed to vary linearly from inlet to exit of the test duct, and is used as the reference temperature to determine the fluid properties. Steady-state convection heat transfer from the internal wall surfaces of the triangular duct to the airflow ($\dot{Q}_c$) can be deduced from the input power ($\dot{E}$) as shown:

$$\dot{Q}_c = \dot{E} - \dot{Q}_r - \dot{Q}_l \tag{2}$$

Rate of conduction heat loss through external surfaces of the whole triangular duct assembly ($\dot{Q}_l$) to the ambient air is estimated by using the Fourier's Law, with the aid of the temperature drop across the duct wall. Radiation heat loss ($\dot{Q}_r$) through both ends of the triangular duct to its surroundings is estimated by the following equation:

$$\dot{Q}_r = \sigma A_c F \varepsilon_r (T_s^4 - T_\infty^4) \tag{3}$$

where view factor between the duct and its surrounding (F) is taken to be unity, and the surface emissivity (ε_r) is measured to be 0.1 by using a Minolta infrared spot thermometer. Convection heat transfer as obtained from Eq. (2) is then counter checked with the internal energy increased by the airflow as shown in the following Eq. (4) to ensure its accuracy:

$$\dot{Q}_c = \dot{m} C_p (T_{ao} - T_{ai}) \tag{4}$$

Hydraulic diameter of the triangular duct ($D = \frac{4\times\text{Flow area}}{\text{Perimeter}}$) is chosen as the characteristic dimension to define Reynolds number and Nusselt number:

$$Re_D = \frac{\rho U D}{\mu} = \frac{U \cdot D}{v} \tag{5}$$

$$Nu_D = \frac{h \cdot D}{k} \tag{6}$$

The friction factor in fully developed turbulent duct flow can be obtained from pressure drop along the test duct and mean velocity of the airflow as shown:

$$f = \frac{\Delta P (D/L)}{2\rho U^2} \tag{7}$$

To describe quantitatively the effects of flow condition and roughness characteristics, namely, Reynolds number (Re_D), Prandtl number (Pr), relative rib height (H/D) and relative rib-to-rib spacing (S/W) on forced convection heat transfer between the horizontal triangular duct and the airflow, Nusselt number is related as:

$$Nu_D = f_1(Re_D, Pr, H/D, S/W) \tag{8}$$

In Eq. (8), the Prandtl number (Pr), which should be an important parameter affecting the heat and mass transfer of the triangular duct, is defined as:

$$Pr = \frac{C_P \mu}{k} \tag{9}$$

However, Prandtl number has not been separately considered in present investigation since air is only used and its Prandtl number in the considered temperature range (T_a: ranging from 300 to 320 K) remains almost constant ($Pr = 0.707$). Hence, Eq. (8) is simplified as:

$$Nu_D = f_2(Re_D, H/D, S/W) \tag{10}$$

Similarly, a relationship for the friction factor (f) of a turbulent flow through a horizontal equilateral triangular duct can then be proposed for its generalization in term of Reynolds number (Re_D), relative rib height (H/D) and relative rib-to-rib spacing (S/W) as shown below:

$$f = f_3(Re_D, H/D, S/W) \tag{11}$$

5. Results and discussions

5.1. Effect of relative rib height (H/D)

To investigate the effect of relative rib height on forced convection and flow friction of a fully developed turbulent flow in a triangular duct with ribbed internal surfaces, representative experimental data obtained with square-sectional ribs ($H = W$) of different sizes but all at a constant rib-to-rib spacing of 57 mm are presented in Fig. 4 over a wide range of Reynolds number from 4000 to 23,000. To facilitate comparison, experimental results obtained from a similar triangular duct with smooth internal surfaces in the previous study [19] are also provided on the same diagram. It can be seen that application of ribs on internal surfaces is able to enhance forced convection in a triangular duct significantly but also leads to a much higher friction loss along the test duct, which agrees well with the previous studies [1–5]. It is because the existence of ribs promotes local turbulence at the duct's surfaces and hence enhances the forced convection. In addition, it can be observed from Fig. 4(a) and (b) that enhancement in both forced convection and flow friction varies with the relative rib height. In order to examine clearly the effect of relative rib height, variations of Nu_D and f against H/D are shown graphically in Fig. 5, at a constant Reynolds number of 10,400 and a rib-to-rib spacing of 57 mm.

It is clearly seen in Fig. 5(a) that an optimum H/D corresponding to a maximum forced convection is observed at 0.18. In fact, as the rib gets larger, the cross-sectional area for the flow decreases, which leads to a higher effective flow velocity and a larger heat transfer area, and thus a higher convection heat transfer. Simultaneously, the sudden-contraction in flow area due to the application of larger ribs also leads to a higher pressure-loss, as a result, the flow friction in the triangular duct increases rather linearly with the relative rib height as shown in Fig. 5(b). A higher flow friction reduces the strength of the secondary flow, which dominates the flow field between ribs, and thus provides a negative effect on the thermal performance of the ribbed-triangular duct. Because of these conflicting effects, the Nusselt number is first increased when the H/D increases, and then decreases as H/D is becoming too large.

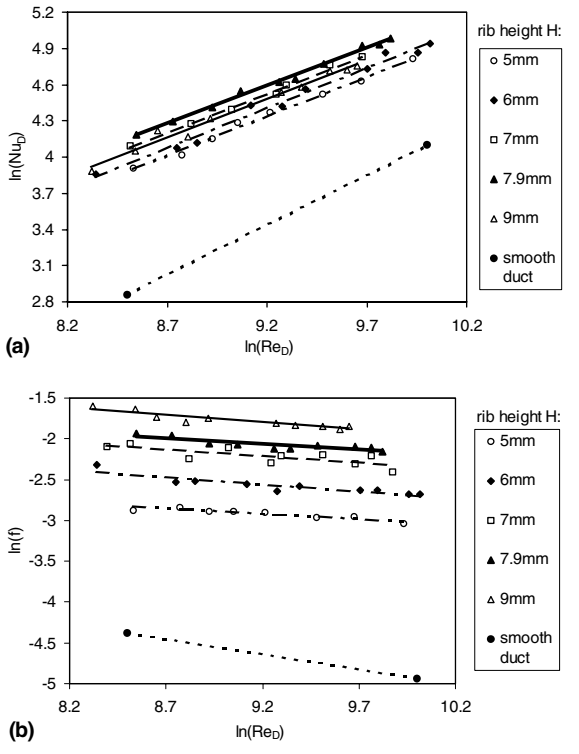

Fig. 4. (a) Variation of experimentally measured Nusselt number with Reynolds number for square ribs of different heights. (b) Variation of experimentally measured friction factor with Reynolds number for square ribs of different heights.

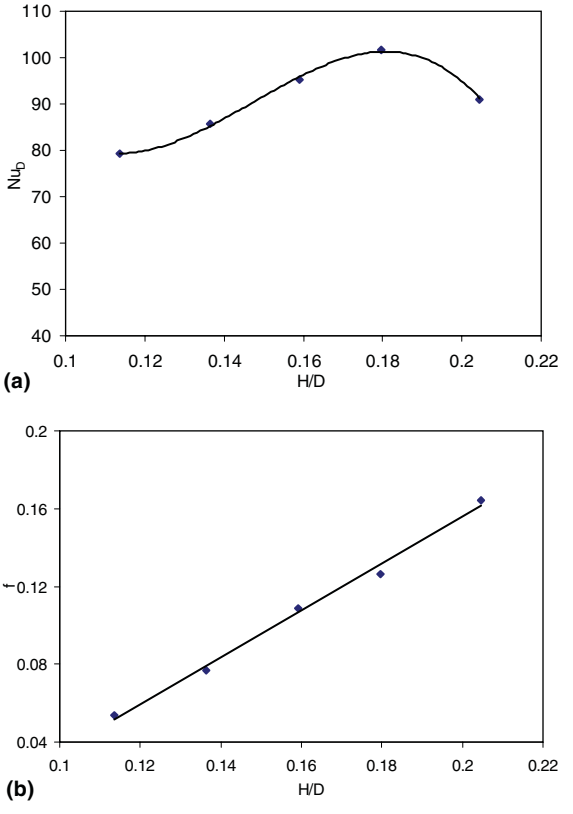

Fig. 5. (a) Variation of experimentally measured Nusselt number with relative rib heights ($Re_D = 10{,}400$, $S = 57$ mm). (b) Variation of experimentally measured friction factor with relative rib heights ($Re_D = 10{,}400$, $S = 57$ mm).

To evaluate the overall performance of the triangular duct with ribbed internal surfaces, it is necessary to consider the forced convection heat transfer and flow friction characteristics simultaneously. Fig. 6(a) shows the performance evaluation of the ducts using the 'volume goodness factor' [20]. The evaluation includes the comparison of the standard pumping power per unit heat transfer area (E_s) and the heat transfer coefficient (h). The standard condition is defined as a condition at 20 °C under atmospheric pressure, and E_s can be expressed as following:

$$E_s = \frac{\dot{m}\Delta p}{\rho A} \tag{12}$$

From Fig. 6(a), it can be found that for the same value of E_s, benefit in applying the rib height of 7.9 mm, which is equivalent to the relative rib height (H/D) of 0.18, becomes rather obvious.

5.2. Effect of relative rib-to-rib spacing (S/W)

Effect of relative rib-to-rib spacing on forced convection and flow friction of the ribbed triangular duct is presented in Fig. 7. Experimental data are obtained with a constant rib size of 7.9 mm × 7.9 mm but at different rib-to-rib spacing ranging from 27 to 110 mm. Similar plots of Nu_D against Re_D, and f against Re_D are made for Re_D = 4000–23,000. As shown in these diagrams, it can be found that effect of relative rib-to-rib spacing (S/W) on both forced convection and flow friction is similar to that of the relative rib height (H/D), except that the variations in both Nu_D and f are not so significant.

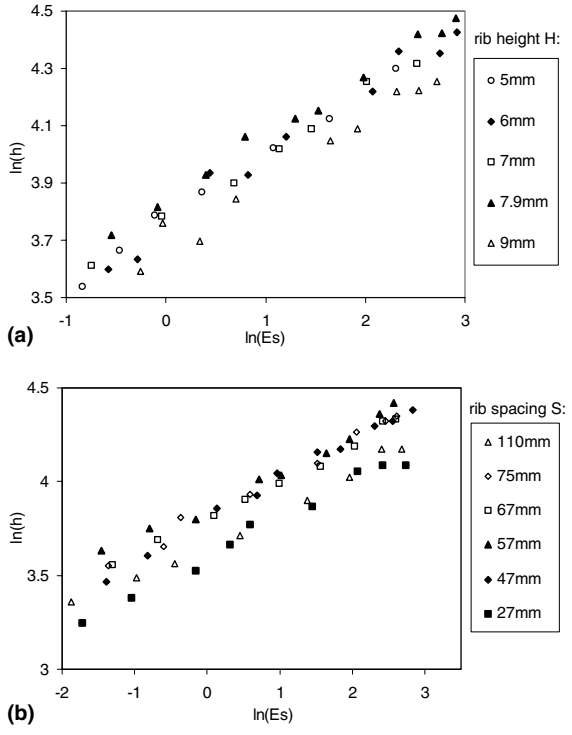

Fig. 6. (a) Comparing heat transfer and pumping power between different rib sizes. (b) Comparing heat transfer and pumping power between different rib-to-rib spacing.

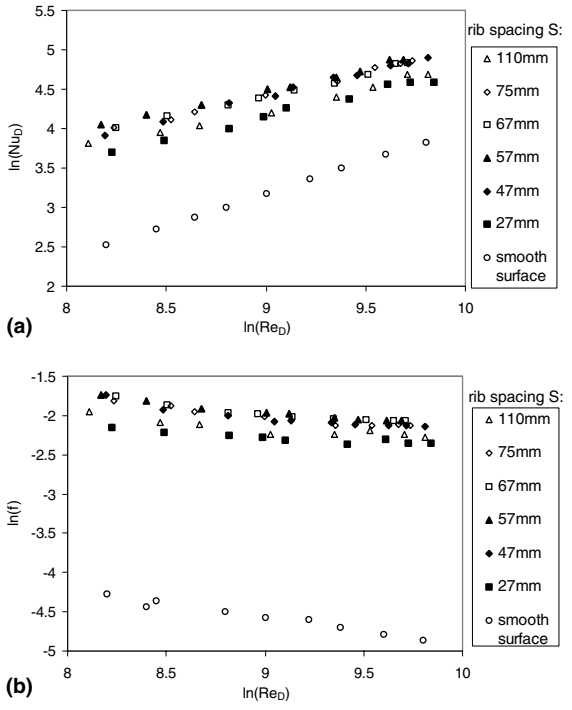

Fig. 7. (a) Variation of experimentally measured Nusselt number with Reynolds number for different rib-to-rib spacing. (b) Variation of experimentally measured friction factor with Reynolds number for different rib-to-rib spacing.

Similarly, to clearly observe the effect of relative rib-to-rib spacing on forced convection and flow friction of the triangular duct, the experimental data are rearranged in the plots of Nu_D against S/W, and f against S/W, as shown in Fig. 8, at a constant Reynolds number of 10,400 and a relative rib height of 0.18. An optimum relative rib-to-rib spacing can be observed at 7.22 corresponding to a maximum Nusselt number, as presented in Fig. 8(a). In addition, Nusselt number is able to maintain around its maximum value for quite a wide range of relative rib-to-rib spacing, which gives a larger flexibility in choosing a suitable rib-to-rib spacing in application.

A similar variation in flow friction with the relative rib-to-rib spacing to that of Nusselt number is observed, both of them obtain their maximum values at S/W = 7.22, as shown in Fig. 8(b). However, the fluctu-

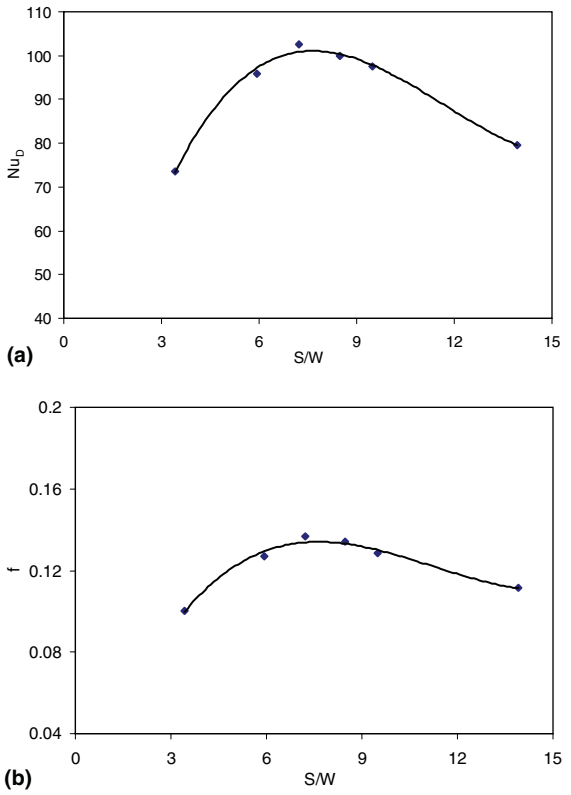

Fig. 8. (a) Variation of experimentally measured Nusselt number with relative rib-to-rib spacing (Re_D = 10,400, H/D = 0.18). (b) Variation of experimentally measured friction factor with relative rib-to-rib spacing (Re_D = 10,400, H/D = 0.18).

ation of flow friction is smaller. An evaluation using the 'volume goodness factor' is also conducted, as shown in Fig. 6(b). It can be observed that the relative rib-to-rib spacing of $S/W = 7.22$ should be a preferred choice to achieve a good balance between heat transfer enhancement and flow friction loss.

All experimental data presented in Figs. 4–8 are rearranged with the least-square method.

5.3. Uncertainty analysis

Uncertainty analysis for Reynolds number, Nusselt number and friction factor in present experimental study have been carried out, respectively. There are several sources of uncertainty caused by different aspects including experimental set-up, instrumentation and measurements of relevant parameters: air temperature (T_a), wall surface temperature (T_s) and pressure drop (ΔP) along the test duct and mass flow rate of air. Since the experimental set-up is well designed and instrumentation involved including thermocouples, pitot tube and manometers have been well pre-calibrated, the major uncertainty comes from measurements of the above parameters. Typically, a maximum uncertainty associated with the mean Reynolds number is determined to be less than ±8%, and the most influential parameter involved is the mass flow rate. For the average Nusselt number, the uncertainty analysis indicates that a maximum uncertainty is ±3% while discrepancy between the calculated and experimental values is only ±2%. Similarly, a maximum uncertainty of ±12% and a discrepancy of ±11% between the calculated and experimental values are observed for the friction factor. Procedures used to estimate the experimental uncertainties are described by Montgomery [21].

6. Non-dimensional expressions for Nusselt number and friction factor

There are two non-dimensional equations developed from the present experimental results: average Nusselt number (Nu_D) and average friction factor (f) in relation to Reynolds number (Re_D), relative rib height (H/D) and relative rib-to-rib spacing (S/W), as shown in Eqs. (10) and (11). A similar approach as described in [5] has been applied.

6.1. Generalization for average Nusselt number

All experimentally obtained average Nusselt numbers are plotted against their corresponding Reynolds numbers and presented in Fig. 9(a). The following relationship is achieved by the least-square method:

$$Nu_D = A_0 Re_D^{A_1} \tag{13}$$

The constant A_1 is found to be 0.5924 and the constant A_0 is a function of the other two involved parameters: H/D and S/W.

To investigate the relationship of relative rib-to-rib spacing (S/W) with Nusselt number (Nu_D), ($Nu_D/Re_D^{A_1}$) is plotted against (S/W) as shown in Fig. 9(b). A polynomial line is achieved with a second-order quadratic equation in the following form:

$$\ln(Nu_D/Re_D^{A_1}) = B_0 + B_1 \ln(S/W) + B_2[\ln(S/W)]^2 \tag{14}$$

The constants B_1 and B_2 are determined to be 1.8414 and −0.4684, respectively, whereas the constant B_0 is a function of the last involved parameter: H/D.

Finally, to reveal the relationship between relative rib height (H/D) and Nusselt number (Nu_D),

$$\left(\frac{Nu_D}{Re_D^{A_1} \left(\frac{S}{W}\right)^{B_1} \left[\exp\left\{ B_2 \left(\ln\left(\frac{S}{W}\right) \right)^2 \right\} \right]} \right)$$

is plotted against (H/D) as shown in Fig. 9(c). The following equation is obtained to fit these points well:

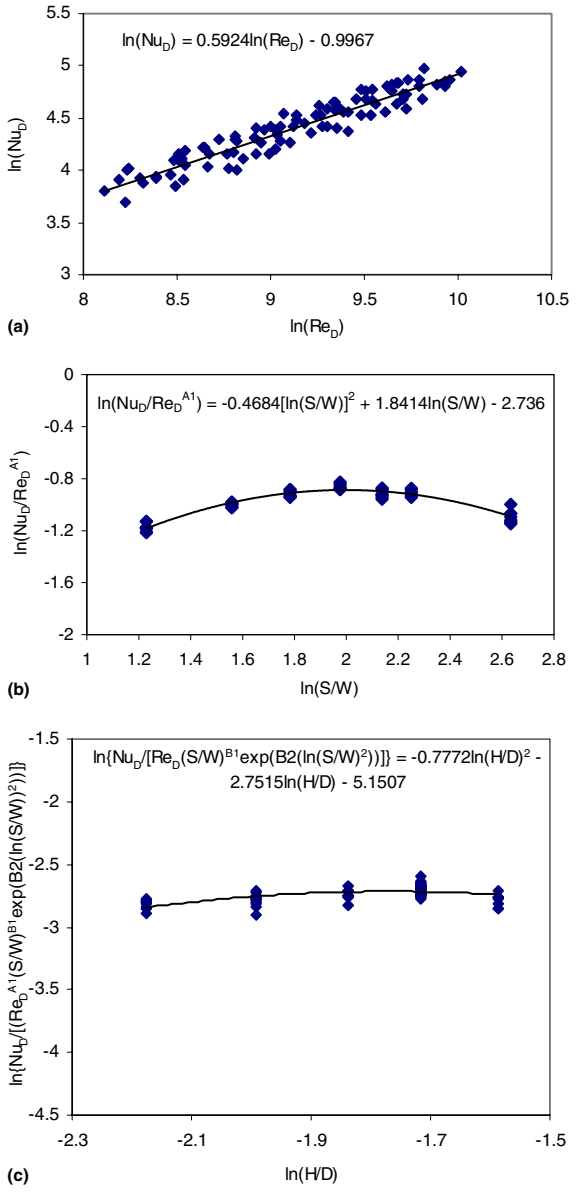

Fig. 9. (a) Variation of Nusselt number with Reynolds number. (b) Plot of $\ln(Nu_D/Re_D^{A_1})$ against $\ln(S/W)$. (c) Plot of $\ln\{Nu_D/[Re_D^{A_1}(S/W)^{B_1}\exp(B_2(\ln(S/W)^2))]\}$ against $\ln(H/D)$.

$$\ln\left(\frac{Nu_D}{Re_D^{A_1}\left(\frac{S}{W}\right)^{B_1}\exp\left\{B_2\left(\ln\left(\frac{S}{W}\right)\right)^2\right\}}\right) = C_0 + C_1\ln(H/D) + C_2[\ln(H/D)]^2 \quad (15)$$

The constants C_0, C_1 and C_2 are determined to be -5.1507, -2.7515 and -0.7772, respectively.

Then, a non-dimensional relationship between Nu_D, Re_D, H/D and S/W is obtained as follows:

$$Nu_D = 0.0058Re_D^{0.5924}\left(\frac{H}{D}\right)^{-2.7515}\left(\frac{S}{W}\right)^{1.8414} \times \exp\left\{-0.7772\left(\ln\left(\frac{H}{D}\right)\right)^2\right\} \times \exp\left\{-0.4684\left(\ln\left(\frac{S}{W}\right)\right)^2\right\} \quad (16)$$

$$\text{for the ranges: } \left\{\begin{array}{l} 4000 \leqslant Re_D \leqslant 23,000 \\ 0.11 \leqslant \dfrac{H}{D} \leqslant 0.21 \\ 3.41 \leqslant \dfrac{S}{W} \leqslant 13.93 \end{array}\right\}$$

6.2. Generalization for average friction factor

A non-dimensional equation for prediction of the average friction factor (f) in terms of Re_D, H/D, S/W is developed by employing the similar procedures. Fig. 10(a–c) depict the stages of obtaining such a relationship in the following form:

$$f = 5.04Re_D^{-0.2897}\left(\frac{H}{D}\right)^{1.6224}\left(\frac{S}{W}\right)^{1.7842} \times \exp\left\{-0.4407\left(\ln\left(\frac{S}{W}\right)\right)^2\right\} \quad (17)$$

$$\text{for the ranges: } \left\{\begin{array}{l} 4000 \leqslant Re_D \leqslant 23,000 \\ 0.11 \leqslant \dfrac{H}{D} \leqslant 0.21 \\ 3.41 \leqslant \dfrac{S}{W} \leqslant 13.93 \end{array}\right\}$$

From the expressions for S/W in Eqs. (16) and (17), respectively, namely,

$$Nu_D \propto \left(\frac{S}{W}\right)^{1.8414}\exp\left(-0.4684\left(\ln\left(\frac{s}{W}\right)\right)^2\right) \text{ and}$$

$$f \propto \left(\frac{S}{W}\right)^{1.7842}\exp\left(-0.4407\left(\ln\left(\frac{s}{W}\right)\right)^2\right)$$

it can be found that Nusselt number (Nu_D) and friction factor (f) have very similar variations with relative rib-to-rib spacing (S/W): both increase first with the increasing S/W and then decrease with lager S/W. However, for the relative rib height (H/D), the situation is quite different: Nu_D obtains its maximum value at an optimum H/D (=0.18), but f increases rather linearly with H/D, which is a big drawback to the enhancement of heat transfer performance of the ribbed triangular duct by increasing the H/D ratio. Moreover, because of the complicated construction of the triangular duct under consideration, the effect of Reynolds number on forced convection of this thermal system ($Nu_D \propto Re_D^{0.5924}$ and $f \propto Re_D^{-0.2897}$) is

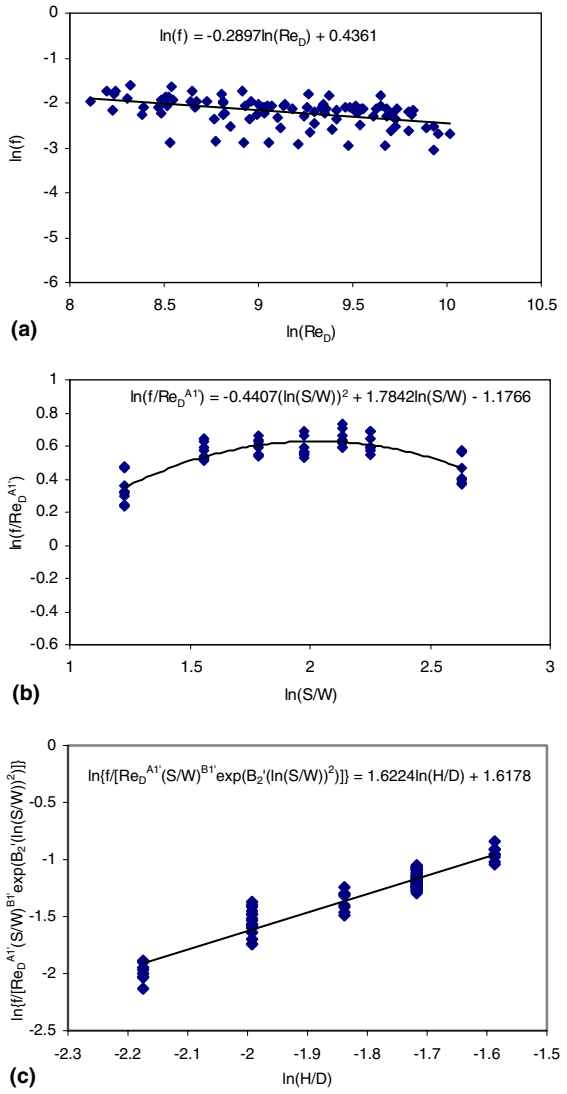

Fig. 10. (a) Variation of friction factor with Reynolds number. (b) Plot of $\ln\left(f/Re_D^{A_1'}\right)$ against $\ln(S/W)$. (c) Plot of $\ln\{f/[Re_D^{A_1'}(S/W)^{B_1'}\exp(B_2'(\ln(S/W)^2))]\}$ against $\ln(H/D)$.

not so significant as it does in a similar smooth triangular duct ($Nu_D \propto Re_D^{0.83}$ and $f \propto Re_D^{-0.37}$) [19]. Considering these three factors' effects on this thermal system, it is observed that when the flow becomes highly turbulent, effect of Reynolds number (Re_D) is more obvious than that of the duct geometry (H/D and S/W). It can be deduced that the attachment of ribs on the internal surfaces of a triangular duct to enhance its heat transfer will be more effective when Reynolds number of the turbulent flow is relative low.

In addition, comparisons between the experimentally obtained Nusselt numbers and friction factors and those

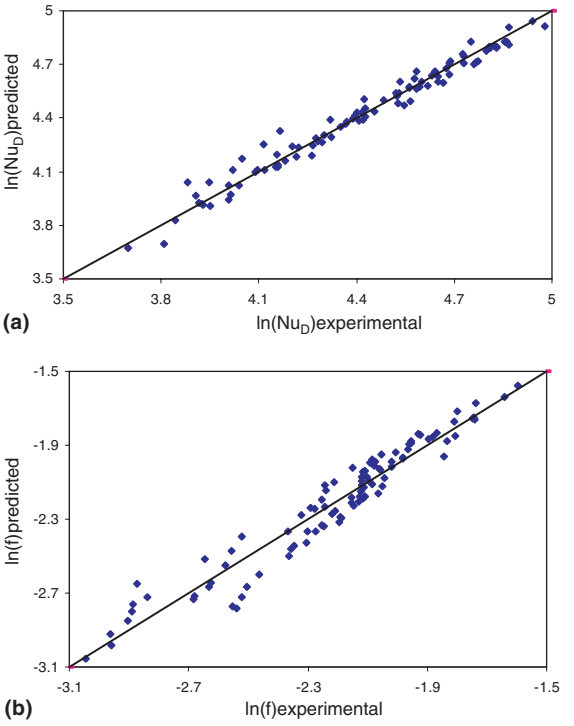

Fig. 11. (a) Plot of experimental and predicted values of Nusselt number. (b) Plot of experimental and predicted values of friction factor.

predicted by Eqs. (16) and (17) are represented in Fig. 11. It can be seen that the predicted Nu_D and f agree very well with the experimental Nu_D and f. Error estimations have been carried out, the maximum percentage deviations between the experimental and predicted values are found to be ±3.5% and ±8.7% for Nu_D and f, respectively.

7. Conclusions

The present study has focused on the investigations of forced convection and flow friction characteristics of a steady-state turbulent flow in a horizontal air-cooled equilateral triangular duct with ribbed internal surfaces. Based on the experimental results obtained, effects of relative rib height and relative rib-to-rib spacing on heat transfer performance of such thermal systems under various Reynolds numbers can be concluded as follow:

- Application of the roughened internal surfaces by fixing uniformly spaced ribs can significantly enhance the forced convection heat transfer between the

turbulent flow and the triangular duct, but it also causes a big drawback of a higher axial pressure drop along the triangular duct.

- The relative rib height (H/D) of 0.18 is proposed to be the optimum rib size corresponding to a maximum forced convection from the heated duct to the airflow. However, the pressure drop along the triangular duct due to flow friction increases almost linearly with the H/D ratio.
- The optimum relative rib-to-rib spacing (S/W) to enhance the forced convection is obtained at 7.22, which leads to a maximum convection heat transfer from the heated duct to the airflow. However, the pressure drop along the triangular duct does not vary linearly with the relative rib-to-rib spacing. A maximum friction loss is also obtained at the relative rib-to-rib spacing of 7.22.
- Non-dimensional relationships for average Nusselt number (Nu_D) and average friction factor (f) in terms of Reynolds number (Re_D), relative rib height (H/D) and relative rib-to-rib spacing (S/W) have been developed from the experimental results as shown in Eqs. (16) and (17), respectively. The maximum percentage deviations for the two equations are ±3.5% and ±8.7%, respectively.

Acknowledgments

The authors wish to acknowledge the financial support to the present work by CERG of the Hong Kong Research Grant Council and CRG of The Hong Kong Polytechnic University (Project number: PolyU5165/01E).

References

[1] H.J. Kang, T.T. Wong, C.W. Leung, Effects of surface roughness on forced convection and friction in triangular ducts, Exp. Heat Transfer 11 (1998) 241–253.
[2] T. Ohara, T. Yamamoto, H. Fujita, Evaporative heat transfer and pressure drop in a rib-roughened flat channel, ASME/JSME Thermal Eng. Proc. 4 (1991) 399–406.
[3] Y.M. Zhang, W.Z. Gu, J.C. Han, Heat transfer and friction in rectangular channels with ribbed or rib-bed-grooved walls, ASME J. Heat Transfer 116 (1994) 58–65.
[4] Y.M. Hong, S.S. Hsieh, Heat transfer and friction factor measurement in ducts with staggered and inline ribs, ASME J. Heat Transfer 115 (1993) 58–65.
[5] R.P. Saini, J.S. Saini, Heat transfer and friction factor correlations for artificially roughened ducts with expanded metal mesh as the roughness element, Int. J. Heat Mass Transfer 40 (4) (1997) 973–986.
[6] S. Lorenz, D. Mukomilow, W. Leiner, Distribution of the heat transfer coefficient in a channel with periodic transverse grooves, Exp. Thermal Fluid Sci. 11 (1995) 234–242.
[7] E. Sparrow, A. Haji-Sheihk, Laminar heat-transfer and pressure drop in isosceles-triangular, right-triangular and circular-section ducts, ASME J. Heat Transfer 87 (1965) 426–427.
[8] H. Nakamura, S. Hiraoka, I. Yamada, Laminar forced convection flow and heat transfer in arbitrary triangular ducts, Heat Transfer—Japanese Research 1 (1972) 120–122.
[9] K.S. Hurst, C.W. Rapley, Turbulent flow measurements in a 30/60-degree right triangular duct, Int. J. Heat Mass Transfer 34 (3) (1991) 739–748.
[10] J.J. Hwang, C.S. Cheng, Impingement cooling in triangular ducts using an array of side-entry wall jets, Int. J. Heat Mass Transfer 44 (5) (2001) 1053–1063.
[11] F.W. Schmidt, M.E. Newell, Heat transfer in fully developed laminar flow through rectangular and isosceles triangular ducts, Int. J. Heat Mass Transfer 10 (1967) 1121–1123.
[12] G.E. Schneider, B.L. LeDain, Fully developed laminar heat transfer in triangular passages, J. Energy 5 (1981) 15–21.
[13] C.A.C. Altemani, E.M. Sparrow, Turbulent heat transfer and fluid flow in an unsymmetrically heated triangular duct, ASME J. Heat Transfer 102 (1980) 590–597.
[14] S.L. Braga, F.E.M. Saboya, Transport coefficient for triangular ducts, IX Congresso Brasileiro de Engenharia Mecanica, Florianopolis, Brazil, 1987, pp. 33–36.
[15] C.W. Leung, S.D. Probert, Forced-convective turbulent flows through horizontal ducts with isosceles triangular internal cross-sections, Appl. Energy 57 (1) (1997) 13–24.
[16] C.W. Leung, S. Chen, T.T. Wong, S.D. Probert, Enhanced forced-convection from ribbed or machine roughened inner surfaces within triangular ducts, Appl. Energy 69 (2001) 87–99.
[17] F.M. White, Fluid Mechanics, third ed., McGraw-Hill, New York, 1994.
[18] A.M.M. Aly, A.C. Trupp, A.D. Gerrard, Measurements and prediction of fully developed turbulent flow in an equilateral triangular duct, J. Fluid Mech. 85 (1) (1978) 57–83.
[19] C.W. Leung, T.L. Chan, S. Chen, Forced convection and friction in triangular duct with uniformly spaced square ribs on inner surfaces, Heat Mass Transfer 37 (2001) 19–25.
[20] W.M. Kays, A.L. London, Compact Heat Exchangers, third ed., McGraw-Hill, New York, 1984.
[21] D.C. Montgomery, Design and Analysis of Experiments, fifth ed., John Wiley, New York, 2001, Chapter 2.